Blends of Poly(2,6-dimethyl-1,4-phenylene oxide)/ Polyamide 6 Toughened by Maleated Polystyrene-based Copolymers: Mechanical Properties, Morphology, and Rheology

Bo Li,[1] Chaoying Wan,[1] Yong Zhang,[1] Jiliang Ji[2]

[1]*State Key Laboratory of Metal Matrix Composites, School of Chemistry and Chemical Technology, Shanghai Jiao Tong University, Shanghai 200240, People's Republic of China*
[2]*R&D Center of Shanghai Kingfa Science and Technology Co., Ltd., Shanghai 201714, People's Republic of China*

Received 8 January 2009; accepted 22 April 2009
DOI 10.1002/app.30742
Published online 4 November 2009 in Wiley InterScience (www.interscience.wiley.com).

ABSTRACT: Poly(2,6-dimethyl-1,4-phenylene oxide)/ polyamide 6 (PPO/PA6 30/70) blends were impact modified by addition of three kinds of maleated polystyrene-based copolymers, i.e., maleated styrene-ethylene-butylene-styrene copolymer (SEBS-*g*-MA), maleated methyl methacrylate-butadiene-styrene copolymer (MBS-*g*-MA), and maleated acrylonitrile-butadiene-styrene copolymer (ABS-*g*-MA). The mechanical properties, morphology and rheological behavior of the impact modified PPO/PA6 blends were investigated. The selective location of the maleated copolymers in one phase or at interface accounted for the different toughening effects of the maleated copolymer, which is closely related to their molecular structure and composition. SEBS-*g*-MA was uniformly dispersed in PPO phase and greatly toughened PPO/PA6 blends even at low temperature. MBS-*g*-MA particles were mainly dispersed in the PA6 phase and around the PPO phase, resulting in a significant enhancement of the notched Izod impact strength of PPO/PA6 blends from 45 J/m to 281 J/m at the MBS-*g*-MA content of 20 phr. In comparison, the ABS-*g*-MA was mainly dispersed in PA6 phase without much influencing the original mechanical properties of the PPO/PA6 blend. The different molecule structure and selective location of the maleated copolymers in the blends were reflected by the change of rheological behavior as well. © 2009 Wiley Periodicals, Inc. J Appl Polym Sci 115: 3385–3392, 2010

Key words: PPO; PA6; SEBS-*g*-MA; MBS-*g*-MA; ABS-*g*-MA; toughening

INTRODUCTION

Poly(2,6-dimethyl-1,4-phenylene oxide)/polyamide 6 (PPO/PA6) blend is a typical incompatible blend, in which PPO contributes good dimensional stability and water resistance while PA6 contributes good melt processability and solvent resistance.[1,2] Because of the incompatibility and relatively low toughness of PPO and PA6, PPO/PA6 blends have low notched impact strength. Therefore, some impact modifiers, usually elastomers, have been used to toughen PPO/PA6 blends.[3–7] Due to the higher adhesion with PPO/PA6 matrix, the modified elastomers had better toughening effects than the elastomers without modification, i.e., maleated poly (ethylene-1-octene) elastomer (POE-*g*-MA) versus POE and maleated ethylene-propylene-diene-monomer rubber (EPDM-*g*-MA) versus EPDM.[8–10] On the other hand, the morphology of elastomers significantly influenced the toughening effect on the PPO/PA6 blends. It was reported that the network of maleated styrene-ethylene-butylene-styrene copolymer (SEBS-*g*-MA) domain was more effective in stopping the growth of the crazing and shear yields than the individual particles in the PPO/PA6 blends.[9,11]

However, there were little publications about SEBS-*g*-MA toughening PPO/PA6 blends at low PPO content. In this article, the effect of SEBS-*g*-MA on the toughness of PPO/PA6 (30/70) blend was studied in detail. Considering that SEBS-*g*-MA was an elastomer and would largely increase the viscosity of PPO/PA6 blend, maleated methyl methacrylate-butadiene-styrene copolymer (MBS-*g*-MA) with core-hell structure was comparatively studied for enhancing both toughness and processability of PPO/PA6 blend. Impact modification by elastomers often leads to significant decreases of tensile strength and modulus of

Correspondence to: Y. Zhang (yong_zhang@sjtu.edu.cn).
Contract grant sponsor: Funds of Science and Technology Commission of Shanghai Municipality; contract grant number: 06XD14213.
Contract grant sponsor: Shanghai Leading Academic Discipline Project; contract grant number: B202.
Contract grant sponsor: Special Funds of Technological Cooperation (between Qingpu District and Shanghai Jiao Tong University).

© 2009 Wiley Periodicals, Inc.

blends. On comparing with other elastomers, acrylonitrile-butadiene-styrene copolymer (ABS) should have the relatively low impairment on the tensile strength and modulus to PPO/PA6 blend due to the high rigidity of acrylonitrile block chains. Therefore, maleated ABS (ABS-*g*-MA) was introduced into the PPO/PA6 blend for obtaining balanced mechanical properties. On the basis of the analysis of the morphology, the toughening mechanism and rheological behavior of the impact modified PPO/PA6 blends were investigated systemically.

EXPERIMENTAL

Materials

PPO, trademark Iupiace PX100L, was produced by Asahi Kasei Corporation, Japan, with an intrinsic viscosity of 0.47 ± 0.02 dl/g measured in trichloromethane at 25°C. PA6, Ube1013B, was produced by Ube Industries, Ltd., Japan, with a relative viscosity of 2.3. SEBS-*g*-MA, MA 001, was made by Kuraray Company, Japan, with the styrene content of 30 wt % and the MA content of 1.7–2.0 wt %. MBS, EXL-2691, was made by Rohm & Hass Company, with the PS and PMMA content of 40 wt % as shell and the PB content of 60 wt % as core. ABS, PA747S, was made by Chi Mei Corporation, China with melt flow index (MFI) of 0.7 g/min (5 kg, 200°C). MA and dicumyl peroxide (DCP) were made by China National Pharmaceutical Group Corporation with analytical grade reagents.

Preparation of toughened PPO/PA6 blends

PPO was grafted with MA via reactive melt extrusion. Powders of PPO, MA, and DCP were premixed in a homogenizer for 10 min at 70°C. Subsequently the mixture was extruded using a corotating twin-screw extruder ($L/D = 41$, $D = 25$ mm) in a processing temperature range of 180–270°C at a rotating speed of 150 rpm. The same procedure was followed for the preparation of MBS-*g*-MA or ABS-*g*-MA but in a processing temperature range of 180–240°C at a rotating speed of 100 rpm. The grafting reaction was studied by Fourier transform infrared spectroscopy (FTIR) and titration analysis. The grafted MA contents in PPO-*g*-MA, MBS-*g*-MA and ABS-*g*-MA were about 0.7 ± 0.1 wt %, 0.5 ± 0.1 wt % and 0.7 ± 0.1 wt %, respectively.

PA6, PPO, PPO-*g*-MA, SEBS-*g*-MA, MBS-*g*-MA, and ABS-*g*-MA were firstly dried at 80°C under vacuum for 12 h and premixed for 5 min. The mixture was then extruded following the same procedure as mentioned before. The processing temperature range was set as 240–260°C, and the screw speed was 200 rpm. The extruded blend was dried in a vacuum oven at 80°C for 12 h before injection molding. Standard tensile and notched Izod impact specimens were prepared according to the ASTM D 638 Type I and ASTM D 256 in a plastic injection molding machine. The barrel temperature was set as 240–260°C, and the mold temperature was 80°C. The injection pressure was set at 40 MPa, whereas the holding pressure was 30 MPa. The holding time and cooling time were 10s and 20s, which could make sure the materials in the cavity, pressurized until cooling down. In this article, all investigations were based on the same content of PPO-*g*-MA and PPO in the blends, which would be denoted as PPO altogether for simplicity and then the weight ratio of PPO/PA6 was fixed to be 30/70 (phr).

Characterization

Mechanical properties tests

Tensile (ASTM D638 Type I) and flexural (ASTM D790) properties were measured using an Instron 4465 universal testing instrument at crosshead speeds of 50 and 2 mm/min, respectively. Notched Izod impact strength (ASTM D256) was measured using 63.5 × 12.7 × 3.2 mm^3 specimens with a V-shape notch on a Ray-Ran universal pendulum impact tester. The hammer speed was 3.5 m/s, and the pendulum weight was 0.818 kg.

Scanning electron microscopy

Scanning electron microscopy (SEM, Hitachi-S-2150, Japan) and field emission scanning electron microscopy (FESEM JSM-7401F, JEOL Co., Japan) were used to observe the fracture surface. The fracture surfaces were etched with trichloromethane for 6 h at room temperature to dissolve PPO and PPO-*g*-MA. The etched and unetched samples were kept in vacuum for 8 h at 80°C and coated with a thin gold layer before observation.

Transmission electron microscopy

The morphology of the blends was investigated by means of transmission electron microscopy (TEM, H-800, Japan) operating at an accelerating voltage of 120 kV. The samples were ultra-microtomed at room temperature to a section in 80–100 nm thickness. The section was stained by OsO_4 for 20 min.

Dynamic mechanical thermal analysis

A dynamic mechanical thermal analyzer (DMTA IV, Rheometric Scientific Inc.) was used to study the thermal mechanical properties of toughened PPO/PA6 blends. Samples were in the form of rectangular strips in dimensions of 10 × 4 × 1 mm^3. The experiment was performed at 1 Hz with a stretching ratio of 0.01%. The sample was first cooled to −100°C and then heated to 220°C at a heating rate of 3°C/min.

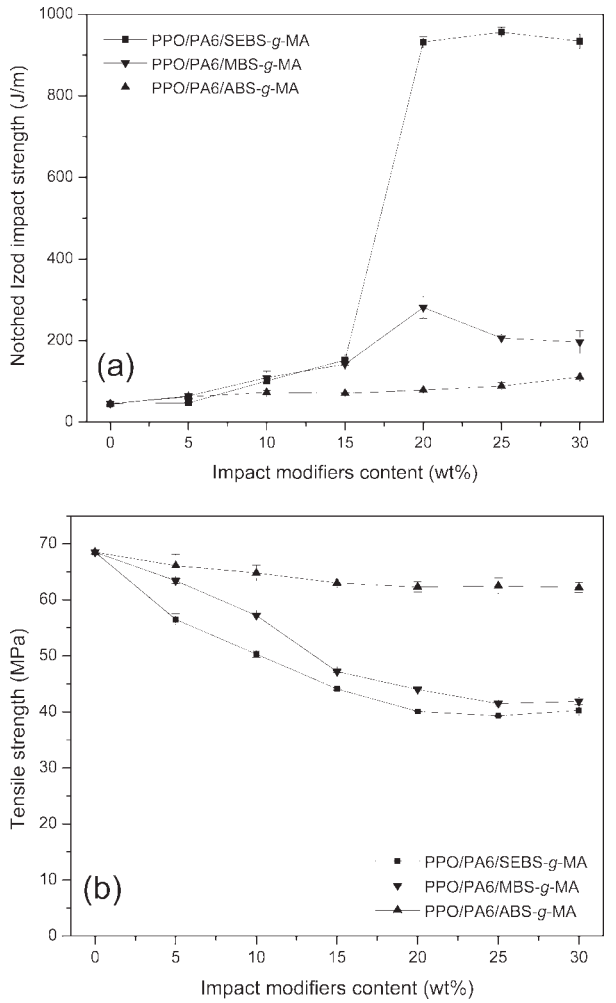

Figure 1 Mechanical properties of PPO/PA6(30/70)/ impact modifiers blends: (a) impact strength, (b) tensile strength.

Capillary rheological measurements

Melt viscosity was measured using an Instron 4467 capillary rheometer (Instron Corp., USA) at 260°C, with a capillary length/diameter ratio of 40/1 and an entrance angle of 180°. The Rabinowitch and Bagley corrections were applied to all the experimental data.

MFI

MFI was measured according to ASTM D1238 using a melt flow indexer (RAY-RAN Test Equipment Ltd., UK) at 250°C and 2.16 kg.

RESULTS AND DISCUSSION

Mechanical properties

Mechanical properties of PPO/PA6 blends toughened by SEBS-*g*-MA, MBS-*g*-MA, and ABS-*g*-MA, respectively, are shown in Figure 1. The notched Izod impact strength of PPO/PA6/SEBS-*g*-MA blends was the highest among the three blends, and it dramatically increased with increasing SEBS-*g*-MA content. As the SEBS-*g*-MA content increased from 15 phr to 20 phr, the blends exhibited a brittle-ductile transition. When the SEBS-*g*-MA content was 20 phr, the blend showed a super-tough behavior with a notched Izod impact strength of 932 J/m as compared with the original value of 45 J/m for the PPO/PA6 blend. This toughening effect could be basically attributed to the good flexibility of the block chains of EB in SEBS-*g*-MA. The notched Izod impact strength of PPO/PA6/MBS-*g*-MA blends increased rapidly with increasing MBS-*g*-MA content and achieved the maximum value of 281 J/m at the MBS-*g*-MA content of 20 phr. Further increasing MBS-*g*-MA content led to a decrease of notched Izod impact strength. The ABS-*g*-MA was less efficient for the increase of the notched Izod impact strength of PPO/PA6 blends as compared with the SEBS-*g*-MA and MBS-*g*-MA. But it was found that the addition of ABS-*g*-MA improved the toughness without sacrificing the tensile strength of PPO/PA6 blend. In comparison, the tensile strength of PPO/PA6 blends toughened by SEBS-*g*-MA or MBS-*g*-MA sharply decreased with increasing impact modifier content. As shown in Figure 1(b), the tensile strength of PPO/PA6/SEBS-*g*-MA and PPO/PA6/MBS-*g*-MA blends dropped from 69.5 MPa to 40.3 MPa and 41.9 MPa, respectively.

The micrographs of fracture surfaces of blends are shown in Figure 2. The PPO/PA6 (30/70) blend itself showed a layered surface with clear and smooth rims in Figure 2(a). A few holes were observed on the fracture surface, which was ascribed to the dispersed phase. For the PPO/PA6 blend with 20 phr SEBS-*g*-MA, the thread-like structure was observed and the area of white zone obviously increased, as shown in Figure 2(b). The high toughness of the PPO/PA6/SEBS-*g*-MA blends was attributed to the large-scale plastic deformation corresponding to the macroscopic stress-whitening during the impact test. When the blend was toughened by 20 phr MBS-*g*-MA, smooth layered surface and large-scale plastic deformation zone appeared simultaneously after fracture, as shown in Figure 2(c), which was consistent with the limited toughening effect of MBS-*g*-MA on the blend. When the blend was toughened by 20 phr ABS-*g*-MA, no large-scale plastic deformation zone occurred and the layered surface became a little fine after fracture, which indicated the poor toughening effect of ABS-*g*-MA on the PPO/PA6 blend.

Notched Izod impact strength of blends at low temperature is illustrated in Figure 3. In the testing temperature range, the notched Izod impact strength of PPO/PA6 blends with the SEBS-*g*-MA content less than 15 phr was lower than 170 J/m. With

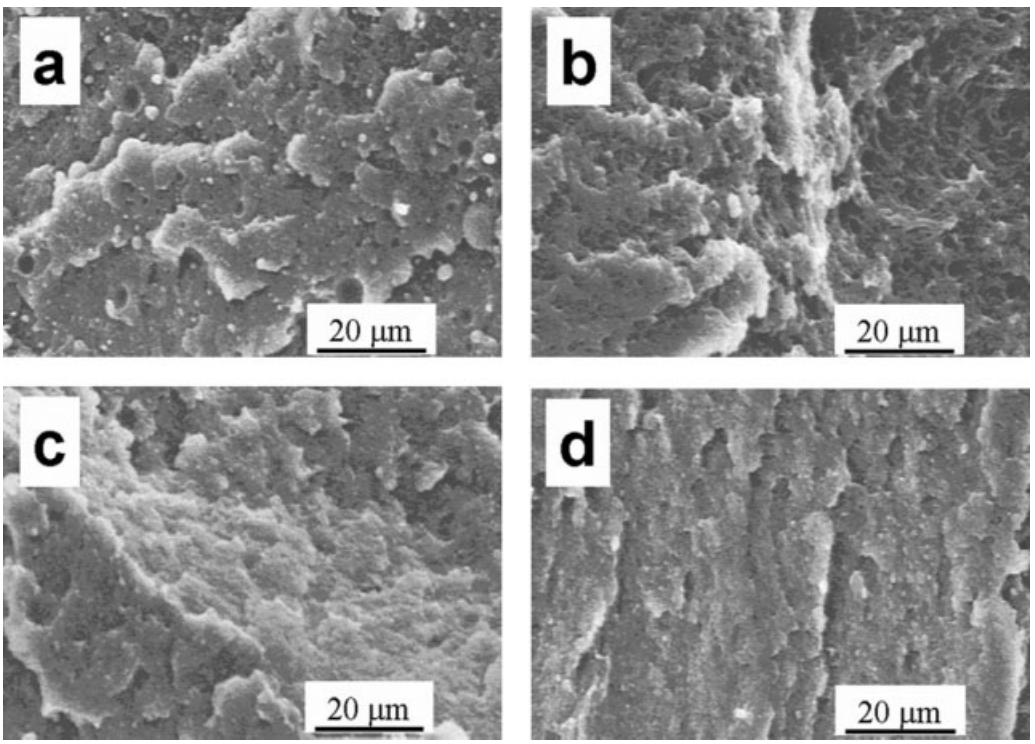

Figure 2 SEM micrographs of fracture surfaces of PPO/PA6/impact modifiers blends at weight ratio of: (a) PPO/PA6 = 30/70, (b) PPO/PA6/SEBS-*g*-MA = 30/70/20, (c) PPO/PA6/MBS-*g*-MA = 30/70/20, (d) PPO/PA6/ABS-*g*-MA = 30/70/20.

further increasing SEBS-*g*-MA content, a brittle-ductile transition occurred in the temperature range from −30°C to −15°C and at temperatures higher than −15 °C, and the blends showed super-tough behavior with the notched Izod impact strength over 500 J/m. In the testing temperature range, the notched Izod impact strength of PPO/PA6 toughened by MBS-*g*-MA or ABS-*g*-MA was relatively low and exhibited a sharp decrease to the value lower than 150 J/m from room temperature to 0°C.

The dynamic mechanical properties of blends such as storage modulus (G') and loss factor (tan Δ) are shown in Figure 4. In the temperature range from 20°C to 110°C, the G' of PPO/PA6/ABS-*g*-MA blends close to the G' of the PPO/PA6 blend was significantly higher than that of PPO/PA6/SEBS-*g*-MA and PPO/PA6/ABS-MA blends. The reason might be that ABS-*g*-MA has higher rigidity than SEBS-*g*-MA and MBS-*g*-MA. It has been reported that the α, β, γ transitions of PPO were about 210, 500, and −100°C, respectively.[12,13] For the PPO/PA6 blend, a tan Δ peak appeared at about 32°C was observed, which should be due to the glass transition of PA6. The glass transition temperature (T_g) of PPO could not be detected since its T_g of 215°C was close to the melting point (T_m) of PA6 of 220°C. When the PPO/PA6 blend was toughened by SEBS-*g*-MA, the tan Δ peak at about −40°C should be due to the glass transition of soft chain segments of SEBS-*g*-MA. However, the other two kinds of toughened blends did not show sharp transitions at low temperatures. That explained why the PPO/PA6 blends toughened by SEBS-*g*-MA had higher notched Izod impact strength at low temperature. For the PPO/PA6/ MBS-*g*-MA blends, there was a small tan Δ peak at about −55°C due to the glass transition of soft chain segments of MBS-*g*-MA. For the PPO/PA6/ABS-*g*-MA blends, the glass transition of soft chain segments was hard to be identified from the DMA spectra. The reason might be that the high rigid acrylonitrile block chains largely reduced the mobility of soft chains of ABS-*g*-MA. On the other hand, the glass transition of rigid chains of ABS-*g*-MA was so strong that we could observe an obvious tan Δ peak at 112°C, whereas SEBS-*g*-MA and MBS-*g*-MA presented weak tan Δ peaks at 93 and 90°C, respectively.

Morphology and toughening mechanism

To investigate the toughening mechanism of PPO/PA6 blends, the morphology of blends was observed by TEM, as shown in Figure 5. The grayish and the black regions corresponded to the PPO phase and the EB or B block chains of impact modifiers, respectively. SEBS-*g*-MA was selectively located in the PPO phase, as shown in Figure 5(a). PPO/SEBS-*g*-MA was dispersed uniformly in the matrix because of the existence of reactive group MA and the blend showed a kind of cocontinuous morphology, which

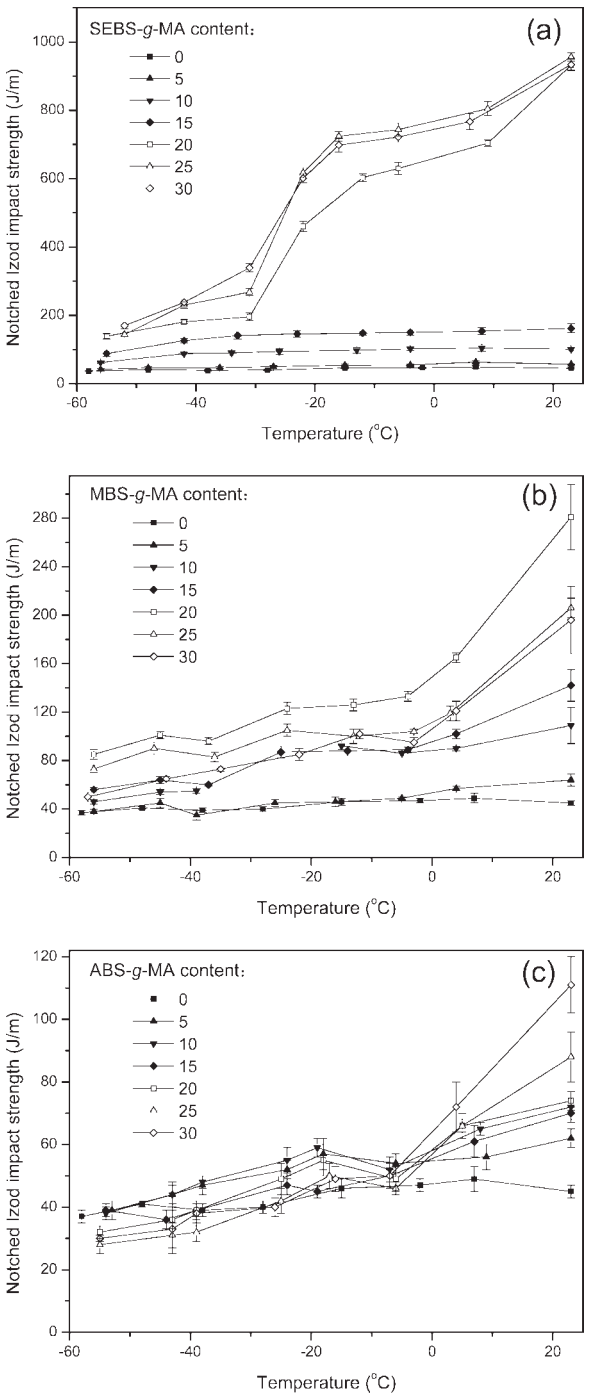

Figure 3 Notched Izod impact strength of PPO/PA6/impact modifiers blends at different temperatures: (a) PPO/PA6/SEBS-*g*-MA, (b) PPO/PA6/MBS-*g*-MA, (c) PPO/PA6/ABS-*g*-MA.

might be due to the high melt viscosity of SEBS-*g*-MA. As seen from Figure 5(b), a large number of spherical particles of MBS-*g*-MA were dispersed around the PPO phase, and the other independent MBS-*g*-MA particles were dispersed easily to aggregate in the PA6 phase. ABS-*g*-MA was dispersed mainly in the PA6 phase, as shown in Figure 5(c). On comparing with other two kinds of impact modifiers, ABS-*g*-MA in the blends preferred aggregation, which did not help to the toughening.

To further investigate the toughening effect of SEBS-*g*-MA, MBS-MA, and ABS-MA on the PPO/PA6 blend, the fracture surface morphology of the blends was observed by SEM (Fig. 6). Fracture surfaces were etched with trichloromethane. Trichloromethane was a good solvent for PPO but a nonsolvent for PA6. PPO had little deformation after fracture in the PPO/PA6 (30/70) blend [Fig. 6(a)], which did not help to absorb the impact energy. That was one reason why the PPO/PA6 blend had low impact strength. When the PPO/PA6 blend was toughened by SEBS-*g*-MA, the large-scale deformation of PPO phase occurred along the impact direction after fracture, as shown in Figure 6(b). PPO was compatible with SEBS-*g*-MA, which made the elastic zones in the blends enlarged and the distance between the elastic zones decreased. Furthermore, SEBS-*g*-MA with good intrinsic flexibility (Table I) and continuous phase structure (Fig. 5), could be helpful to transfer the impact energy and induce the plastic deformation of the matrix, results in the super toughness.

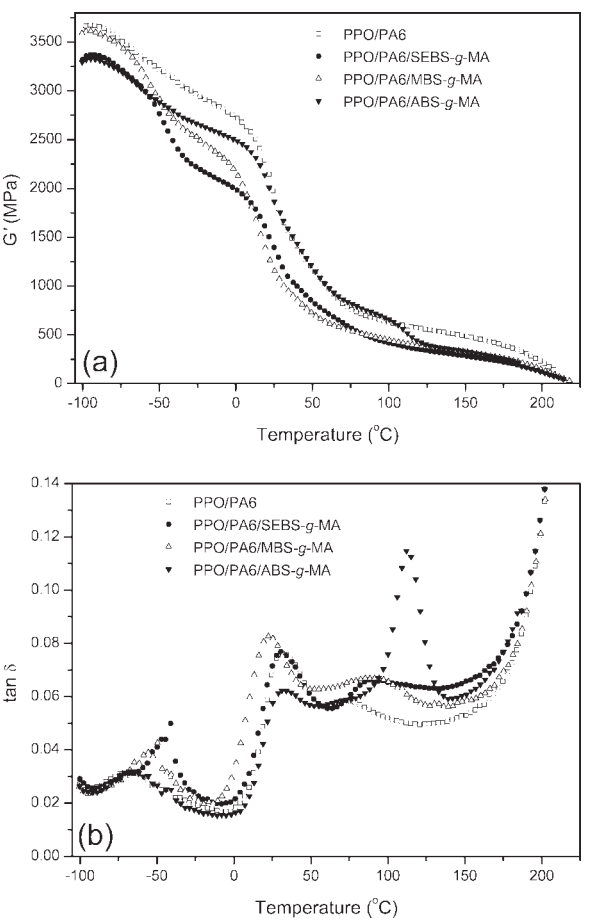

Figure 4 (a) Storage modulus and (b) Loss factor of PPO/PA6 (30/70) blend and PPO/PA6/impact modifiers (30/70/20) blends.

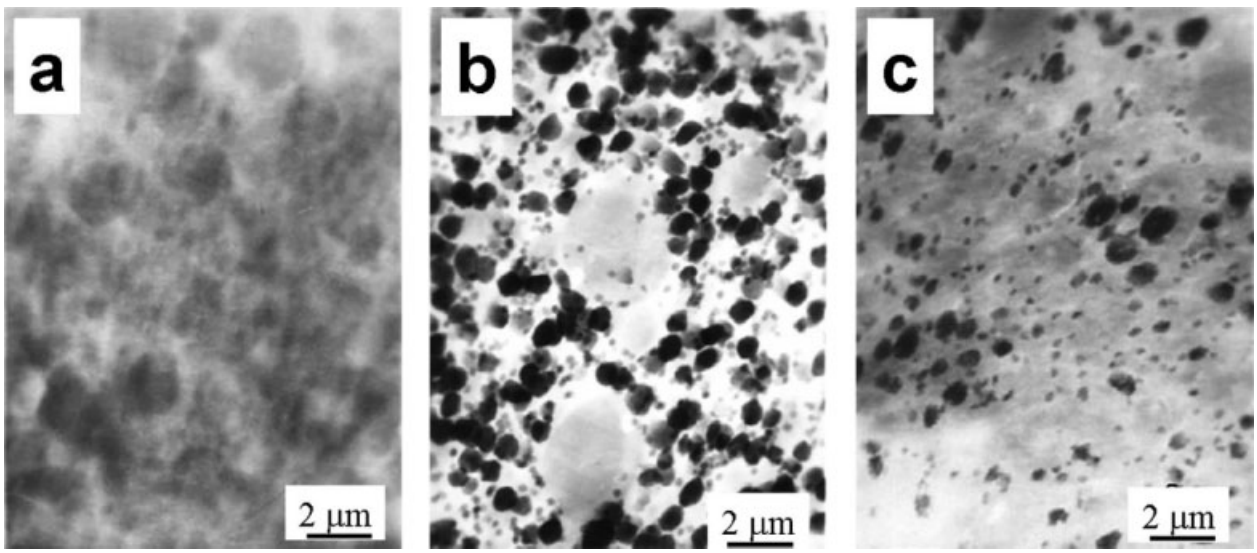

Figure 5 TEM micrographs of PPO/PA6/impact modifiers (30/70/30) blends: (a) SEBS-*g*-MA, (b) MBS-*g*-MA, (c) ABS-*g*-MA.

According to the percolation model,[14] to achieve the good flexibility, the SEBS-MA content should be less than the content of other impact modifiers. In Figure 6(c), some cavities left by etching parts were elongated along the impact direction to a certain extent. As seen in Figure 5(b), a large number of MBS-*g*-MA particles were dispersed around the PPO phase. During the impact fracture, the deformation of these MBS-*g*-MA particles might urge the deformation of the PPO phase to absorb the impact energy. At the same time, MBS-*g*-MA particles with their small dimension might urge the tiny cracks and also restrict the development of tiny cracks into macro cracks. These factors might explain why notched Izod impact strength of MBS-*g*-MA was low (86 J/m), but its toughening effect on the blend was great and notched Izod impact strength of PPO/PA6/MBS-*g*-MA blends could reach the maximum value of 281 J/m (Table I). As seen in Figure 6(d), the cavities had little

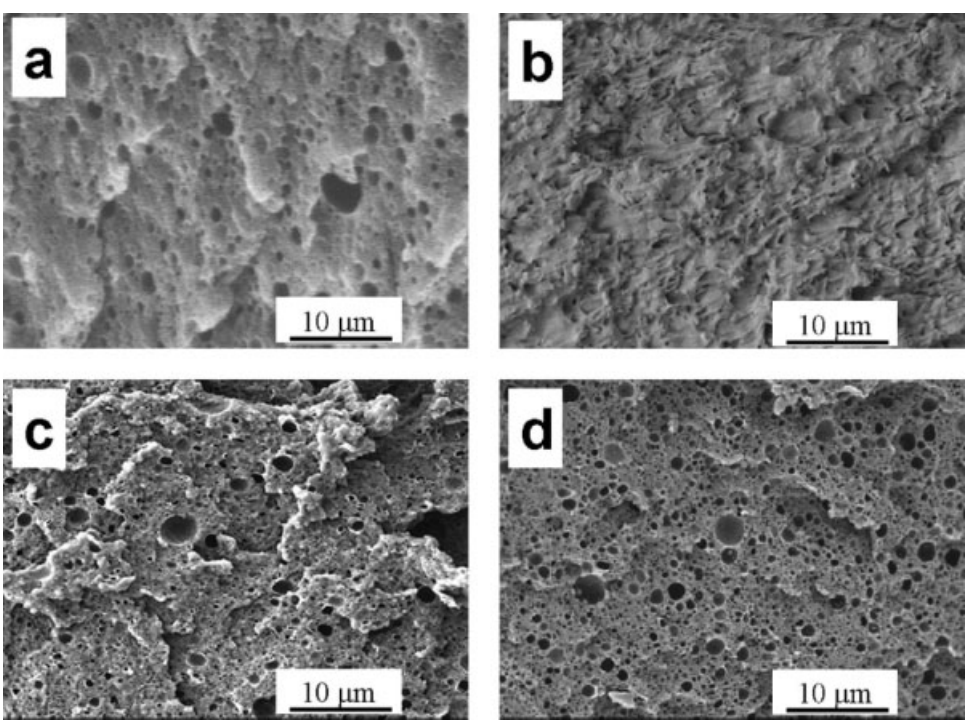

Figure 6 SEM micrographs of fracture surfaces of PPO/PA6/impact modifiers blends etched with trichloromethane at weight ratio of: (a) PPO/PA6 = 30/70, (b) PPO/PA6/SEBS-*g*-MA = 30/70/20, (c) PPO/PA6/MBS-*g*-MA = 30/70/20, (d) PPO/PA6/ABS-*g*-MA = 30/70/20.

TABLE I
Notched Izod Impact Strength of Materials

sample	Notched Izod impact strength (J/m)
PPO	63
PA6	69
PPO/PA6[a]	45
SEBS-*g*-MA	N. B.[b]
PPO/PA6/SEBS-*g*-MA[a]	956[c]
MBS-*g*-MA	86
PPO/PA6/MBS-*g*-MA[a]	281[c]
ABS-*g*-MA	356
PPO/PA6/ABS-*g*-MA[a]	111[c]

[a] The weight ratio of PPO/PA6 was 30/70, the PPO represented PPO-*g*-MA and PPO with equal weight content in this paper.
[b] Not break.
[c] Data was the maximum value in this article.

deformation, which could be attributed to that the ABS-*g*-MA was not well compatible with PPO. Due to the dispersion of ABS-*g*-MA which was mainly in PA6 phase, the deformation of ABS-*g*-MA phase could not effectively induce the deformation of PPO phase (dispersed phase) during the impact fracture. So the absorbance of impact energy was limited. Although the notched Izod impact strength of ABS-*g*-MA was high (356 J/m), the toughening effect of ABS-*g*-MA on the PPO/PA6 blend was poor and the blends showed the typical brittleness with the maximum value of the notched Izod impact strength of 111 J/m (Table I).

Rheology

The viscosity of blends shown in Figure 7 was measured in the capillary rheometer at 260°C. The viscosity of the PPO/PA6/SEBS-*g*-MA(ABS-*g*-MA) blends significantly increased with increasing impact modifier content because of the high melt viscosity of the

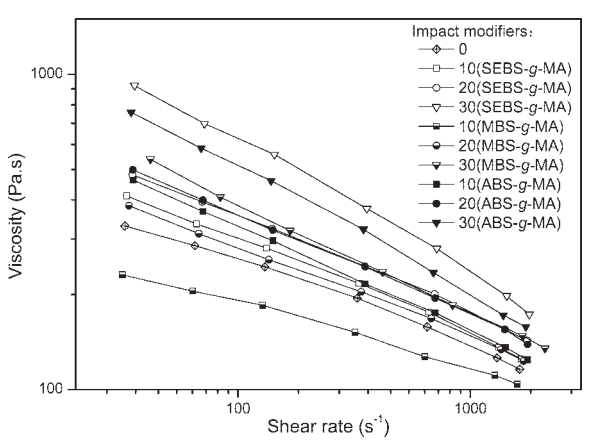

Figure 7 Capillary rheological curves for the PPO/PA6/impact modifiers blends.

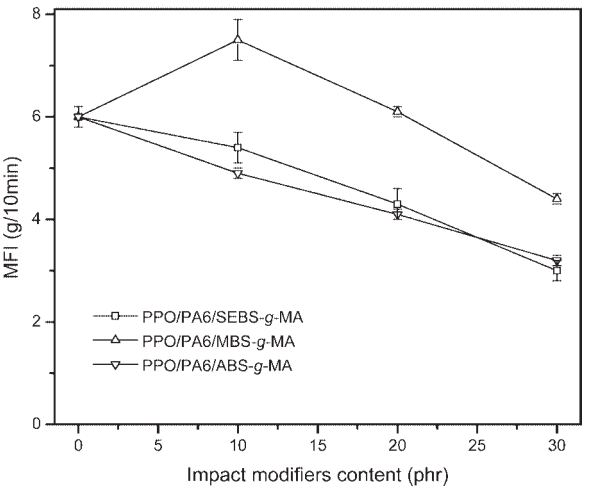

Figure 8 The effect of the impact modifiers content on the MFI of the PPO/PA6/impact modifiers blends.

impact modifiers. Accordingly, their MFI decreased with increasing impact modifier content (Fig. 8). In comparison, the viscosity of the PPO/PA6/MBS-*g*-MA blends obviously decreased and then increased with increasing MBS-*g*-MA content. The viscosity of polymer melts depends on the interlayer interaction, hence interlayer slip or inhomogeneous flow may account for the decrease in viscosity.[15] On comparing with SEBS-*g*-MA and ABS-*g*-MA, MBS-*g*-MA has core-hell structure and intrinsic low viscosity. Thus, the independent spherical MBS-*g*-MA particles with small dimension might serve as "ball bearing" so that the viscosity of the PPO/PA6/MBS-*g*-MA blends decreased. However, at the high content of MBS-*g*-MA, the reaction between MBS-*g*-MA and amine groups of PA6 would definitely increase the viscosity of PPO/PA6/MBS-*g*-MA. Then the MFI of the blends would decrease with increasing MBS-*g*-MA content (higher than10 phr).

At high share rate, the viscosity versus share rate can be approximated as:

$$\eta = k\gamma^{n-1} \tag{1}$$

$$\log \eta = \log\ k + (n-1)\log\ \gamma \tag{2}$$

where η is viscosity, $n-1$ represents the slope of curve which depict the relationship between the log η and log γ at high share rate.[16] From Figure 7, the power law index n could be calculated and the results were summarized in Table II. With the increasing impact modifiers content, the n of PPO/PA6/SEBS-*g*-MA(ABS-*g*-MA) blends decreased and led to more remarkable shear-thinning behavior, which could be due to the easily tangling ability of the long and soft chains of the impact modifiers. The n of PPO/PA6/MBS-*g*-MA blends slightly increased and then decreased with increasing MBS-*g*-MA

TABLE II
Power Law Index (*n*) of Impact Modified PPO/PA6 Blends

Impact modifiers		SEBS-*g*-MA			MBS-*g*-MA			ABS-*g*-MA		
Content (wt %)	0	9.1	16.7	23.1	9.1	16.7	23.1	9.1	16.7	23.1
n	0.73	0.70	0.69	0.58	0.79	0.72	0.65	0.68	0.66	0.60

content. The spherical MBS-*g*-MA particles might alleviate the tangles of polymer chains.

CONCLUSIONS

The toughening effects of SEBS-*g*-MA, MBS-*g*-MA and ABS-*g*-MA on PPO/PA6 (30/70) blend were influenced largely by the final dispersion of maleated copolymers due to their different composition and molecular structure. The SEBS-*g*-MA was well compatible with PPO, and the formed PPO/SEBS-*g*-MA phase could be dispersed well in PA6 matrix due to its reactions with PA6. Subsequently, SEBS-*g*-MA showed the best toughening effect on the PPO/PA6 blend. In the PPO/PA6/MBS-*g*-MA blends, the MBS-*g*-MA particles were distributed in the PA6 phase and around the PPO phase. The toughening effect of MBS-*g*-MA on PPO/PA6 blend might be due to following factors: (i) MBS-*g*-MA particles had deformation after fracture for their elastic block chains, (ii) some PPO particles surrounded with MBS-*g*-MA particles elongated to a certain extent along impact direction, (iii) MBS-*g*-MA particles with small dimension might arrest the cracks or at least reduce their propagation. ABS-*g*-MA was not well compatible with PPO and led to the poor toughening effect on PPO/PA6 blend. MBS-*g*-MA serving as "ball bearing" had the ability to decrease the viscosity of the blends. At the same time, the disentanglement of polymer chains caused by the addition of MBS-*g*-MA could weaken the shear-thinning behavior of the blends.

References

1. Ji, Y. L.; Li, W. G.; Ma, J. H. Macromol Rapid Commun 2005, 26, 116.
2. Li, Y. L.; Xie, T. X.; Yang, G. S. J Appl Polym Sci 2006, 99, 2076.
3. van der Meer; Hobbs, S. Y. EP0236593, 1987.
4. Son, Y.; Lee, S. Polym Bull 2006, 56, 267.
5. Chiou, K. C.; Wu, S. C.; Wu, H. D.; Chang, F. C. J Appl Polym Sci 1999, 74, 23.
6. Yates, J. B. III. EP0550210, 1992.
7. Gianchandai, J. K.; Hasson, A.; Wroczynski, R. J.; Yates, J. B. III. EP0550206, 1993.
8. Wang, X. D.; Feng, W.; Li, H. Q. J Appl Polym Sci 2003, 88, 3110.
9. Wu, D. Z.; Wang, X. D.; Jin, R. G. Eur Polym J 2004, 40, 1223.
10. Tjong, S. C.; Ke, Y. C. Eur Polym J 1998, 34, 1565.
11. Wu, D. Z.; Wang, X. D.; Jin, R. G. J Appl Polym Sci 2006, 99, 3336.
12. Nanasawa, A.; Takayama, S.; Takeda, K. J Appl Polym Sci 1997, 66, 19.
13. Judit, E. P.; Kwon, Y.; Altstädt, V.; Kontopoulou, M. Polymer 2007, 48, 590.
14. Margolina, A.; Wu, S. Polymer 1988, 29, 2170.
15. Mackay, M. E.; Henson, D. J. J Rheol 1998, 42, 1505.
16. Han, C. D. Rheology and Processing of Polymeric Materials; Oxford University Press, New York, 2007, p 204.